Hindawi
Advances in Mathematical Physics
Volume 2018, Article ID 3586514, 17 pages
https://doi.org/10.1155/2018/3586514

Research Article

A Newton-Type Approach to Approximate Travelling Wave Solutions of a Schrödinger-Benjamin-Ono System

Juan Carlos Muñoz Grajales

Departamento de Matemáticas, Universidad del Valle, Calle 13 Nro. 100-00, Cali, Colombia

Correspondence should be addressed to Juan Carlos Muñoz Grajales; jcarlmz@yahoo.com

Received 1 October 2017; Revised 1 March 2018; Accepted 13 March 2018; Published 19 April 2018

Academic Editor: Remi Léandre

We introduce a Newton's iterative method to approximate periodic and nonperiodic travelling wave solutions of the Schrödinger-Benjamin-Ono system derived by M. Funakoshi and M. Oikawa. We analyze numerically the influence of the model's parameters on these solutions and illustrate the collision of two unequal-amplitude solitary waves propagating with different speeds computed by using the proposed numerical scheme.

1. Introduction

This paper is concerned with the nonlinear one-dimensional system (hereafter called the Schrödinger-Benjamin-Ono system (SBO))

$$\begin{aligned} i\partial_t u + \partial_x^2 u &= \alpha v u, \\ \partial_t v - \gamma \mathcal{H} \partial_x^2 v &= \beta \left(|u|^2\right)_x, \end{aligned} \tag{1}$$

for $x \in (0, L)$, $t > 0$ with periodic spatial boundary conditions. This nonlinear dispersive system was derived by Funakoshi and Oikawa [1] to describe the motion of two fluids with different densities under capillary-gravity waves in a deep water regime. The functions $u = u(x,t) : \mathbb{R} \times \mathbb{R} \to \mathbb{C}$ and $v = v(x,t) : \mathbb{R} \times \mathbb{R} \to \mathbb{R}$ denote the short and long wave terms, respectively. The parameters α, β, γ are real numbers, and $\mathcal{H}$ denotes the Hilbert transform

$$\mathcal{H} f(x) := \text{p.v.} \frac{1}{\pi} \int \frac{f(y)}{y - x} dy, \tag{2}$$

where p.v. $\int$ stands for the integration in the principal value sense. Other physical scenarios, where system (1) with $\gamma = 0$ arises, are the sonic-Langmuir wave interaction in plasma physics (Karpman [2]), the capillary-gravity interaction waves (Djordjevic and Redekopp [3], Grimshaw [4]), and water-wave interaction in a nonlinear medium (see, e.g., [5, 6]).

Due to a balance between dispersive and nonlinear effects, system (1) admits the so-called *travelling-wave solutions* in the form

$$\begin{aligned} u(x,t) &= e^{iwt} e^{ic(x-ct)/2} \phi(x - ct), \\ v(x,t) &= \psi(x - ct), \end{aligned} \tag{3}$$

where $w, c \in \mathbb{R}$ and ϕ, ψ are periodic real-valued functions or smooth real-valued functions such that, for each $n \in \mathbb{N}$, $\phi^{(n)}(\chi) \to 0$ and $\psi^{(n)}(\chi) \to 0$, as $|\chi| \to \infty$. In this last case, these solutions are called *solitary waves*. In the literature there are some previous analytical results about periodic and nonperiodic travelling wave solutions to the SBO system. For instance, Angulo and Montenegro [7] established the existence of even solitary wave solutions by employing the concentration compactness method (Lions [8, 9]). Existence and stability of a new family of solitary waves was established in [10] for system (1) and a coupled Schrödinger-KdV model. On the other hand, when $|\gamma| \neq 1$, the nonperiodic initial value problem corresponding to the SBO system has been considered by Bekiranov et al. [11], who proved well-posedness in the Sobolev space $H^s_{\mathbb{C}}(\mathbb{R}) \times H^{s-1/2}_{\mathbb{R}}(\mathbb{R})$, with $s \geq 0$. In the case of $|\gamma| = 1$, Pecher [12] showed local well-posedness for $s > 0$, and Angulo et al. [13] proved

global well-posedness for $s = 0$ and $|\gamma| \neq 1$. However, there are only a few results known for the spatial periodic problem. For instance, assuming that $|\gamma| \neq 0, 1$, Angulo et al. [13] showed that system (1) is locally well posed in the Sobolev space $H^s(0, 2\pi) \times H^{s-1/2}(0, 2\pi)$ for $s \geq 1/2$ and they further established existence of a smooth branch of periodic travelling wave solutions of the SBO system for $\gamma \neq 0$ and close to 0, and $w - c^2/4 > 2\pi^2/L^2$, where L is the fundamental period.

In this paper, we introduce a numerical scheme for approximating the periodic and nonperiodic travelling wave solutions of system (1), with $\gamma \neq 0$ whose existence was established in previous works ([7, 10, 13]). This scheme combines a Fourier spectral discretization together with a Newton-type iteration which is initialized by means of well-known exact solutions for the case $\gamma = 0$. By using the spectral Crank–Nicolson numerical scheme introduced in [14] for solving system (1), we validate the approximate travelling waves computed and also illustrate the phenomenon of collision of two right-running unequal-amplitude solitary waves propagating with different speeds. The behavior of the colliding solitary waves is found to be similar to solitary wave solutions of other nonintegrable dispersive-type equations, such as the scalar Benjamin equation [15] and the regularized Benjamin-Ono equation [16]. Such numerical study on the travelling wave solutions of the SBO system has not been considered in previous works to the best knowledge of the author. Furthermore, we obtain numerically new periodic travelling wave solutions which are not included in the analytical theory presented in the work by Angulo et al. [13]. These are the main contributions of the present study. Other contribution is to explain the application of a numerical scheme which belongs to the spectral collocation methods to approximate the solutions of integrodifferential equations, such as system (1). These numerical methods have been intensively used in the solution of dispersive-type equations in the last years. We point out that exact solutions for system (1) are not known when $\gamma \neq 0$. Therefore, a numerical strategy is very important in order to investigate the properties of the solution space, such as to establish the parameter regime for existence of periodic and nonperiodic travelling waves, orbital stability under small initial disturbances, and interactions among these solutions, for example. We point out that the constant γ in the SBO system is positive for physical meaning [1]. However, as we mentioned above, in previous works [7, 10–12], the SBO system has been studied from a mathematical point of view, establishing well-posedness and that travelling wave solutions for the SBO system are possible when the parameter γ takes both signs. This is an interesting mathematical fact, and thus we will conduct some numerical experiments which illustrate the family of travelling wave solutions for both $\gamma > 0$ and $\gamma < 0$.

This paper is organized as follows. In Section 2, we present a brief review of well-known exact solutions of the SBO system for $\gamma = 0$. In Section 3, we explain the numerical methodology used to find approximations to travelling wave solutions of the SBO system. In Section 4, we compute some periodic and nonperiodic travelling wave solutions of the system, analyze the influence of model's parameters on the geometry of periodic and nonperiodic travelling waves, and explore the collision of two right-going solitary waves of the SBO system. Finally, Section 5 contains the conclusions of our work.

2. Computing Exact Travelling Wave Solutions

For the sake of completeness, in this section, we present a brief review of a class of exact travelling wave solutions of system (1) (periodic and non-periodic) which are well known in the literature when $\gamma = 0$ (see [7, 10, 13] for more details and analytical results on existence of travelling wave solutions for $\gamma \neq 0$). These analytical special cases are important because they can be used as initial points for computing branches of solutions when $\gamma \neq 0$, through Newton's iteration and numerical continuation, for example.

In the nonperiodic case and $\gamma = 0$, we can construct a family of exact travelling wave solutions in the form (3) of system (1). In first place, note that, for $\gamma = 0$, the real-valued functions ϕ, ψ must satisfy the system

$$\phi'' + \left(\frac{c^2}{4} - w\right)\phi = \alpha\phi\psi, \tag{4}$$

$$-c\psi' - \beta\left(\phi^2\right)' = 0, \tag{5}$$

where the tildes denote differentiation with respect to the variable $\chi = x - ct$.

We recall that ϕ, ψ and their derivatives decay to zero at infinity. Thus we can integrate (5) to get

$$\psi = -\frac{\beta}{c}\phi^2. \tag{6}$$

After substituting the value of ψ into (4), we obtain

$$\phi'' + \left(\frac{c^2}{4} - w\right)\phi = -\frac{\alpha\beta}{c}\phi^3. \tag{7}$$

By multiplying the previous equation by ϕ', we get

$$\phi'\phi'' = \left(w - \frac{c^2}{4}\right)\phi\phi' - \frac{\alpha\beta}{c}\phi^3\phi'. \tag{8}$$

Therefore,

$$\left(\frac{\phi'^2}{2}\right)' = \left(w - \frac{c^2}{4}\right)\frac{\left(\phi^2\right)'}{2} - \frac{\alpha\beta\left(\phi^4\right)'}{4c}, \tag{9}$$

$$\psi = -\frac{\beta}{c}\phi^2. \tag{10}$$

Thus, by integrating (9) and using again the decaying properties of the functions ϕ, ψ, we obtain

$$\left(\phi'\right)^2 = \left(w - \frac{c^2}{4}\right)\phi^2 - \frac{\alpha\beta}{2c}\phi^4, \tag{11}$$

$$\psi = -\frac{\beta}{c}\phi^2. \tag{12}$$

Looking for solutions of (11) in the form $\phi(\chi) = A\,\mathrm{sech}^s(B\chi)$, where A, B, s are real constants to be determined, we have that

$$\begin{aligned} &A^2B^2s^2\mathrm{sech}\left(B\chi\right)^{2+2s}\sinh^2\left(B\chi\right) \\ &\quad= \left(w - \frac{c^2}{4}\right)A^2\mathrm{sech}^{2s}\left(B\chi\right) - \frac{\alpha\beta}{2c}A^4\mathrm{sech}^{4s}\left(B\chi\right), \end{aligned} \tag{13}$$

or, equivalently,

$$\begin{aligned} &A^2B^2s^2\mathrm{sech}^2\left(B\chi\right)\sinh^2\left(B\chi\right) \\ &\quad= \left(w - \frac{c^2}{4}\right)A^2 - \frac{\alpha\beta}{2c}A^4\mathrm{sech}^{2s}\left(B\chi\right). \end{aligned} \tag{14}$$

Using the identity $\sinh^2(B\chi) = -1 + \cosh^2(B\chi)$, we arrive at

$$\begin{aligned} &-A^2B^2s^2\mathrm{sech}^2\left(B\chi\right) + A^2B^2s^2 + \left(\frac{c^2}{4} - w\right)A^2 \\ &\quad= -\frac{\alpha\beta}{2c}A^4\mathrm{sech}^{2s}\left(B\chi\right). \end{aligned} \tag{15}$$

From this equation we can conclude that

$$\begin{aligned} s &= 1, \\ A^2B^2 &= \left(w - \frac{c^2}{4}\right)A^2. \end{aligned} \tag{16}$$

On the other hand, evaluating (15) at $\chi = 0$,

$$A^2B^2s^2 = \frac{\alpha\beta}{2c}A^4. \tag{17}$$

Substituting the value of the constant B in the previous equation, we arrive at

$$\begin{aligned} A^2 &= \frac{2c}{\alpha\beta}\left(w - \frac{c^2}{4}\right), \\ B^2 &= w - \frac{c^2}{4}. \end{aligned} \tag{18}$$

Therefore,

$$\begin{aligned} \phi\left(\chi\right) &= A\,\mathrm{sech}\left(B\chi\right), \\ \psi\left(\chi\right) &= -\frac{\beta}{c}A^2\mathrm{sech}^2\left(B\chi\right). \end{aligned} \tag{19}$$

On the other hand, in the periodic case and with $\gamma = 0$, we also have that ϕ, ψ must also satisfy system (4)-(5). By integrating (5), we get

$$-c\psi = \beta\phi^2 + A_\psi, \tag{20}$$

where A_ψ is a constant. Here we assume that $A_\psi = 0$. Thus, after substituting this expression for ψ into (4), we arrive at

$$\phi'' + \left(\frac{c^2}{4} - w\right)\phi = -\frac{\alpha\beta}{c}\phi^3. \tag{21}$$

Therefore, we obtain

$$\left(\phi'^2\right)' = \left(w - \frac{c^2}{4}\right)\left(\phi^2\right)' - \frac{\alpha\beta\left(\phi^4\right)'}{2c}. \tag{22}$$

Then integrating the last equation, we arrive at

$$\begin{aligned} \left(\phi'\right)^2 &= \left(w - \frac{c^2}{4}\right)\phi^2 - \frac{\alpha\beta\phi^4}{2c} + B_\phi \\ &= \frac{\alpha\beta}{2c}\left(-\phi^4 + \frac{2c\left(w - \left(c^2/4\right)\right)}{\alpha\beta}\phi^2 + \frac{2cB_\phi}{\alpha\beta}\right), \end{aligned} \tag{23}$$

where B_ϕ is a constant. Suppose that $w > c^2/4$, α, β, c are positive real numbers and B_ϕ is negative. Furthermore, let $\eta_1, \eta_2, -\eta_1, -\eta_2$ ($\eta_1 > 0$, $\eta_2 > 0$) be the roots of the polynomial of the right side of the previous equations; then we can write

$$\left(\phi'\right)^2 = \frac{\alpha\beta}{2c}\left(\eta_1^2 - \phi^2\right)\left(\phi^2 - \eta_2^2\right), \tag{24}$$

and thus

$$\begin{aligned} \left(\phi'\right)^2 &= \frac{\alpha\beta}{2c}\left(-\phi^4 - \eta_1^2\eta_2^2 + \eta_1^2\phi^2 + \phi^2\eta_2^2\right) \\ &= \frac{\alpha\beta}{2c}\left(-\phi^4 + \left(\eta_1^2 + \eta_2^2\right)\phi^2 - \eta_1^2\eta_2^2\right). \end{aligned} \tag{25}$$

Therefore,

$$\begin{aligned} \eta_1^2 + \eta_2^2 &= \frac{2c\left(w - c^2/4\right)}{\alpha\beta}, \\ -\eta_1^2\eta_2^2 &= \frac{2cB_\phi}{\alpha\beta}. \end{aligned} \tag{26}$$

Without less of generality, we may assume that $\eta_1 > \eta_2$, and consider the change of variable $\zeta = \phi/\eta_1$. Substituting (24), we get

$$\begin{aligned} \eta_1^2\left(\zeta'\right)^2 &= \frac{\alpha\beta}{2c}\left(\eta_1^2 - \eta_1^2\zeta^2\right)\left(\eta_1^2\zeta^2 - \eta_2^2\right) \\ &= \frac{\alpha\beta}{2c}\eta_1^2\left(1 - \zeta^2\right)\eta_1^2\left(\zeta^2 - \frac{\eta_2^2}{\eta_1^2}\right). \end{aligned} \tag{27}$$

Let $k^2 = 1 - \eta_2^2/\eta_1^2 = (\eta_1^2 - \eta_2^2)/\eta_1^2$. Thus

$$\left(\zeta'\right)^2 = \frac{\alpha\beta\eta_1^2}{2c}\left(1 - \zeta^2\right)\left(\zeta^2 + k^2 - 1\right). \tag{28}$$

Now let us define $\zeta^2 = 1 - k^2\sin^2\chi$. Then

$$2\zeta\zeta' = -2k^2\sin\chi\cos\chi\chi', \tag{29}$$

and thus

$$\left(\zeta'\right)^2 = \frac{k^4\sin^2\chi\cos^2\chi\left(\chi'\right)^2}{1 - k^2\sin^2\chi}. \tag{30}$$

Substituting this expression into (28), we obtain

$$\frac{k^4\sin^2\chi\cos^2\chi\left(\chi'\right)^2}{1-k^2\sin^2\chi}=\frac{\alpha\beta}{2c}\eta_1^2k^2\sin^2\chi\left(k^2-k^2\sin^2\chi\right). \quad (31)$$

We can simplify the previous equation to get

$$\begin{aligned}\left(\chi'\right)^2&=\frac{\alpha\beta\eta_1^2}{2c}\left(1-k^2\sin^2\chi\right),\\ \chi'&=\sqrt{\frac{\alpha\beta}{2c}}\eta_1\sqrt{1-k^2\sin^2\chi},\\ \frac{d\chi}{\sqrt{1-k^2\sin^2\chi}}&=\eta_1\sqrt{\frac{\alpha\beta}{2c}}d\xi.\end{aligned} \quad (32)$$

Assuming that $\zeta(0)=1$, then $\chi(0)=0$ and integrating the previous equation

$$\int_{\chi(0)}^{\chi(\xi)}\frac{dt}{\sqrt{1-k^2\sin^2t}}=\int_0^{\xi}\eta_1\sqrt{\frac{\alpha\beta}{2c}}d\xi=\eta_1\sqrt{\frac{\alpha\beta}{2c}}\xi=l\xi, \quad (33)$$

where $l=\eta_1\sqrt{\alpha\beta/2c}$. Using from the definition of the Jacobian elliptic function $\mathrm{sn}(u;k)$, we get $\sin\chi=\mathrm{sn}(l\xi;k)$ and hence $\zeta(\xi)=\sqrt{1-k^2\mathrm{sn}^2(l\xi;k)}\equiv\mathrm{dn}(l\xi;k)$. In terms of the original variables ϕ,ψ, we obtain the dnoidal wave solutions corresponding to system (11)-(12):

$$\begin{aligned}\phi(\xi)&=\phi\left(\xi;\eta_1,\eta_2\right)=\eta_1 dn\left(l\xi;k\right)\\ \psi(\xi)&=\psi\left(\xi;\eta_1,\eta_2\right)=-\frac{\eta_1^2\beta}{c}dn^2\left(l\xi;k\right),\end{aligned} \quad (34)$$

where

$$\begin{aligned}k^2&=\frac{\eta_1^2-\eta_2^2}{\eta_1^2},\\ \eta_1^2+\eta_2^2&=\frac{2c\left(w-c^2/4\right)}{\alpha\beta},\\ &0<\eta_2<\eta_1.\end{aligned} \quad (35)$$

Since the fundamental period of the dnoidal function dn is $2K(k)$, where

$$K(k)\equiv\int_0^{\pi/2}\frac{dt}{\sqrt{1-k^2\sin^2t}}, \quad (36)$$

it follows that ϕ has fundamental period T_ϕ given by

$$T_\phi=\frac{2K}{l}=\frac{2K}{\eta_1}\sqrt{\frac{2c}{\alpha\beta}}. \quad (37)$$

We point out that, due to the factor $e^{ic(x-ct)/2}$ in the component $u(x,t)$ of the travelling wave solution (3), we have the condition

$$T_\phi=\frac{2K}{\eta_1}\sqrt{\frac{2c}{\alpha\beta}}=\frac{4\pi}{c}m, \quad (38)$$

for some $m\in\mathbb{N}$.

3. Methodology for Approximation of Travelling Wave Solutions of the Full SBO System

For $\gamma\neq0$, we recall that if (u,v) is a travelling wave solution in the form

$$\begin{aligned}u(x,t)&=e^{iwt}e^{ic(x-ct)/2}\phi(x-ct),\\ v(x,t)&=\psi(x-ct),\end{aligned} \quad (39)$$

of system (1), then ϕ,ψ are real-valued functions which must satisfy the following equations:

$$\begin{aligned}\phi''+\left(\frac{c^2}{4}-w\right)\phi-\alpha\phi\psi&=0,\\ \gamma\mathscr{H}\left(\psi'\right)+c\psi&=-\beta\phi^2.\end{aligned} \quad (40)$$

In first place, we are interested in finding approximations to even solutions (ϕ,ψ) with period $2l$, $l>0$ of system (1); let us introduce truncated cosine expansions for u and v:

$$\begin{aligned}\phi(x)&\approx\phi_0+\sum_{n=1}^{N/2}\phi_n\cos\left(\frac{n\pi}{l}x\right),\\ \psi(x)&\approx\psi_0+\sum_{n=1}^{N/2}\psi_n\cos\left(\frac{n\pi}{l}x\right),\end{aligned} \quad (41)$$

where

$$\begin{aligned}\phi_0&=\frac{1}{l}\int_0^l\phi(x)\,dx=\frac{1}{2l}\int_0^{2l}\phi(x)\,dx,\\ \phi_n&=\frac{2}{l}\int_0^l\phi(x)\cos\left(\frac{n\pi x}{l}\right)dx\\ &=\frac{2}{2l}\int_0^{2l}\phi(x)\cos\left(\frac{n\pi x}{l}\right)dx,\end{aligned} \quad (42)$$

and let us introduce analogous expressions for the coefficients ψ_n. By substituting expressions (41) into (40), evaluating them at the $N/2+1$ collocation points

$$x_j=\frac{2l\left(j-1\right)}{N},\quad j=1,\ldots,\frac{N}{2}+1, \quad (43)$$

and using the property of the Hilbert transform

$$\mathscr{H}\left(e^{ikx}\right)=i\,\mathrm{sign}(k)\,e^{ikx},\quad k\in\mathbb{Z}, \quad (44)$$

we obtain the system of $N+2$ nonlinear equations,

$$\begin{aligned}
&-\sum_{n=1}^{N/2}\left(\frac{n\pi}{l}\right)^2\phi_n\cos\left(\frac{n\pi x_j}{l}\right)\\
&+\left(\frac{c^2}{4}-w\right)\sum_{n=0}^{N/2}\phi_n\cos\left(\frac{n\pi x_j}{l}\right)\\
&-\alpha\left(\sum_{n=0}^{N/2}\phi_n\cos\left(\frac{n\pi x_j}{l}\right)\right)\left(\sum_{n=0}^{N/2}\psi_n\cos\left(\frac{n\pi x_j}{l}\right)\right)\\
&=0,\\
&-\gamma\sum_{n=1}^{N/2}\frac{n\pi}{l}\psi_n\cos\left(\frac{n\pi x_j}{l}\right)+c\sum_{n=0}^{N/2}\psi_n\cos\left(\frac{n\pi x_j}{l}\right)\\
&=-\beta\left(\sum_{n=0}^{N/2}\phi_n\cos\left(\frac{n\pi x_j}{l}\right)\right)^2,
\end{aligned}\tag{45}$$

for $j=1,\ldots,N/2+1$, which can be written in the form

$$F\left(\phi_0,\phi_1,\ldots,\phi_{N/2},\psi_0,\psi_1,\ldots,\psi_{N/2}\right)=0,\tag{46}$$

where the $N+2$ coefficients ϕ_n,ψ_n are the unknowns. We point out that the property (44) of the Hilbert transform makes the numerical solution of system (40) with the spectral collocation proposed in the present paper easier. This is the motivation for the choice of this numerical strategy.

Nonlinear system (46) can be solved by Newton's iteration. Computation of the cosine series in (41) and the integrals in (42) is performed using the FFT (Fast Fourier Transform) algorithm. The Jacobian of the vector field $F:\mathbb{R}^{N+2}\to\mathbb{R}^{N+2}$ is approximated by the second-order accurate formula

$$J_{i,j}F(x)\approx\frac{F_i\left(x+he_j\right)-F_i\left(x-he_j\right)}{2h},\qquad j=1,\ldots,N+2,\tag{47}$$

where $e_j=(0,\ldots,1,\ldots,0)$ and $h=0.01$. We stop Newton's iteration when the relative error between two successive approximations and the value of the vector field F are smaller than 10^{-12}. We use the travelling wave solutions given in Section 2, when $\gamma=0$, for initializing the Newton's iterative scheme explained above.

4. Description and Discussion about the Numerical Results

In the following, we present some numerical experiments performed by using the numerical scheme described in the previous section.

Experiment Set 1 (Periodic Waves). In the first numerical experiment we set $\gamma=\alpha=\beta=1$, $c=0.5$, and $w=1.5$, and the fundamental period is $L=4\pi/c$. The iterative Newton's procedure is initialized with

$$\begin{aligned}
\phi_0(x)&=2\cos\left(\frac{2\pi x}{L}\right),\\
\psi_0(x)&=\cos\left(\frac{2\pi x}{L}\right).
\end{aligned}\tag{48}$$

The result of this computer simulation is presented in Figure 1. To check that we have computed really a periodic travelling wave of the SBO system (1), we run the spectral Crank-Nicolson numerical solver to approximate the solutions to this system, introduced by the author in [14], with time step $\Delta t=10^{-3}$, and $N=2^8$ FFT points; the spatial computational domain is the interval $[0,L]$ with $L=4\pi/c\approx 25.13$, and the initial values are

$$\begin{aligned}
u(x,0)&=e^{icx/2}\phi(x),\\
v(x,0)&=\psi(x),
\end{aligned}\tag{49}$$

with ϕ,ψ being the profiles displayed in Figure 1. The result of this computer simulation at $t=7$ is displayed in Figure 2, superimposed with the expected position of the travelling wave given by (39). We observe a good accordance with a maximum error of 10^{-3} between the profiles of the modulus of components u and v, corroborating that, in fact, we have an approximation of a travelling wave solution to system (1). The same verification was performed successfully for other periodic travelling waves computed for different values of the parameter w, displayed in Figures 3, 4, and 5 for $w=0.5$, $w=0.1$, and $w=0.06$, respectively.

We remark that Angulo et al. in [13] established, by using the concentration compactness method (Lions [8, 9]), the existence of periodic travelling wave solutions of system (1), provided that $w-c^2/4>2\pi^2/L^2$, where L is the fundamental period. Thus, the numerical experiment in Figure 5 with $w=0.06$, $c=0.5$, that is, $w-c^2/4<0$, shows that travelling wave solutions of the SBO system may also exist outside the parameter regime considered in [13]. In Figure 6, we display another numerical simulation with $w=0.06$, $c=1$, where we also obtain an approximate travelling wave solution for $w-c^2/4<0$, by initializing the Newton's iteration with

$$\begin{aligned}
\phi_0(x)&=4\cos\left(\frac{2\pi x}{L}\right),\\
\psi_0(x)&=\cos\left(\frac{2\pi x}{L}\right).
\end{aligned}\tag{50}$$

In Figure 7, we show new periodic travelling waves of system (1) for $\gamma\neq 0$ computed by using as initial step for Newton's iteration the periodic solutions obtained in (34), corresponding to the case $\gamma=0$. In this experiment we use the model's parameters $\alpha=\beta=1$, $\gamma=1$, $c=1.5$, and $w=1.5$. Given the parameters α,β,c, the values of the parameters η_1,η_2,k

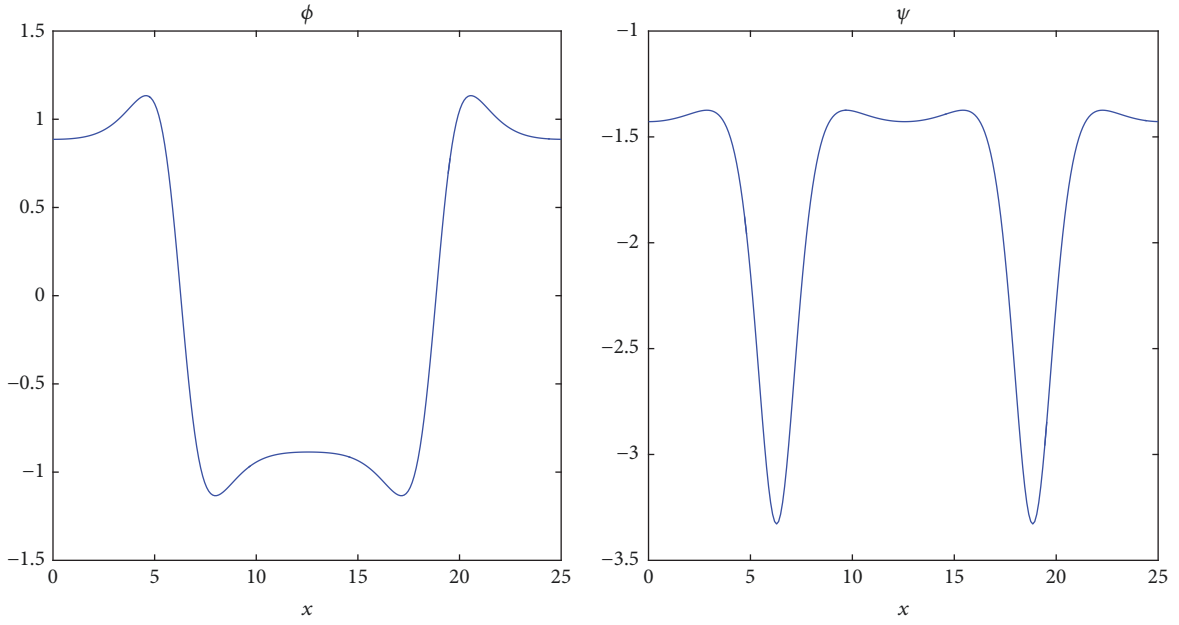

Figure 1: Approximations of the functions ϕ, ψ in the travelling wave solution (39) with 9 Newton's iterations. The model's parameters are $\alpha = \beta = \gamma = 1$, $w = 1.5$, and wave speed $c = 0.5$ and the fundamental period is $L \approx 25.13$.

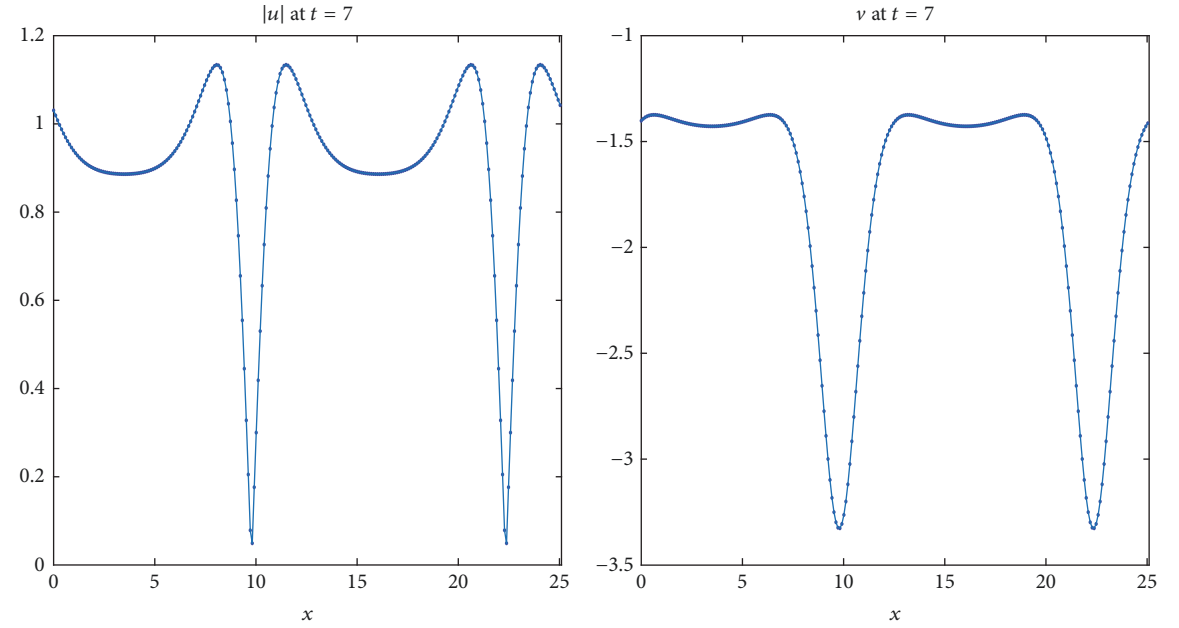

Figure 2: Evolution of the travelling wave solution (39) (with ϕ, ψ as in Figure 1) of the SBO system at $t = 7$. In solid line, $|u|, v$ computed with the numerical solver introduced in [14]. In pointed line, $|u|, v$ for the approximate travelling wave solution (39).

are approximated numerically satisfying the relationships obtained in Section 2:

$$\eta_1 = \sqrt{\frac{2c\left(w - c^2/4\right)}{\alpha\beta} - \eta_2^2},$$
$$\frac{2K\left(\sqrt{\left(\eta_1^2 - \eta_2^2\right)/\eta_1^2}\right)}{\eta_1}\sqrt{\frac{2c}{\alpha\beta}} - \frac{4\pi}{c} = 0. \tag{51}$$

In this case, the results are $\eta_1 \approx 1.6729$, $\eta_2 \approx 0.1175$, and $k \approx 0.9975$. The resulting fundamental period of the travelling wave is $L = 4\pi/c \approx 8.37$.

In Figure 8, we show the computation of other periodic travelling wave of the SBO system with $\gamma = 1 \neq 0$, using as initial step in Newton's scheme the periodic solution (34) with the parameters $\alpha = \beta = 0.5$, $c = 2$, and $w = 2$. Again, the parameters η_1, η_2, k are approximated numerically and the results are $\eta_1 \approx 3.9328$, $\eta_2 \approx 0.7297$, and $k \approx 0.9826$. Thus the

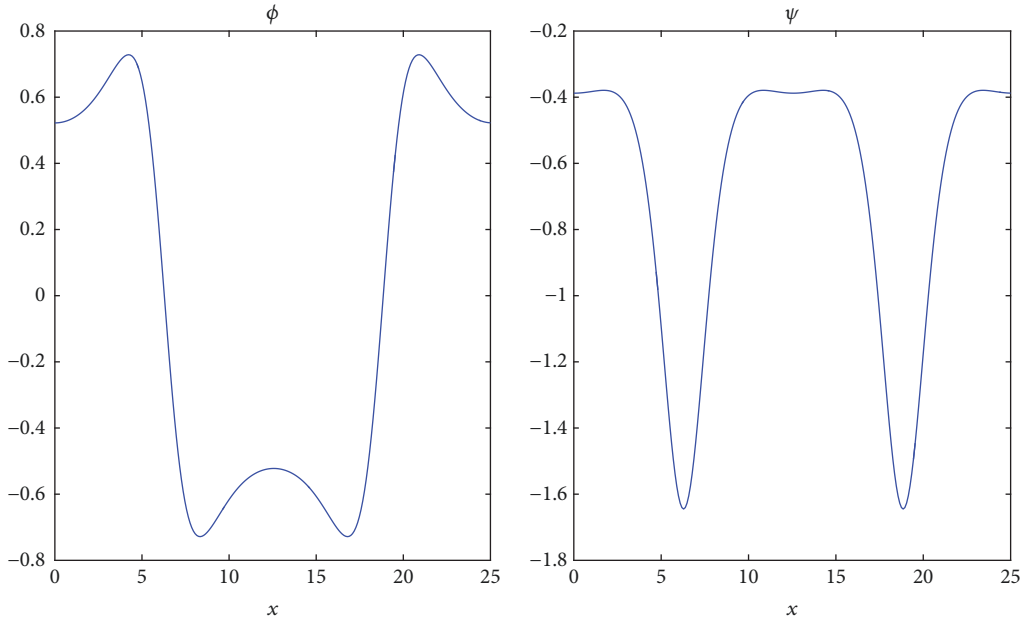

Figure 3: Approximations of the functions ϕ, ψ in the travelling wave solution (39) with 10 Newton's iterations. The model's parameters are $\alpha = \beta = \gamma = 1$, $w = 0.5$, and wave speed $c = 0.5$ and the fundamental period is $L \approx 25.13$.

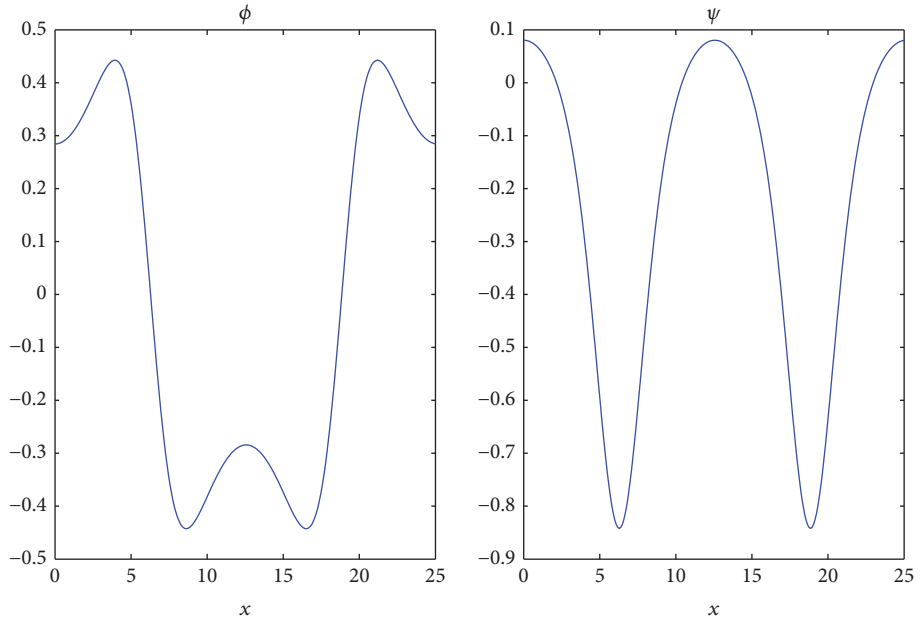

Figure 4: Approximations of the functions ϕ, ψ in the travelling wave solution (39) with 11 Newton's iterations. The model's parameters are $\alpha = \beta = \gamma = 1$, $w = 0.1$, and wave speed $c = 0.5$ and the fundamental period is $L \approx 25.13$.

resulting fundamental period of the travelling wave is $L = 4\pi/c \approx 6.28$. We point out that, in this numerical simulation, the travelling wave is faster ($c = 2$) than the one computed in the previous numerical experiment ($c = 1.5$).

It is important to remark that the first purpose of the previous numerical experiments is to show that the proposed Newton-pseudospectral scheme can be used to approximate with good accuracy and low computational cost, travelling-wave solutions of the SBO system. This fact was corroborated for every travelling wave computed (see, e.g., Figure 2), where we see that the corresponding wave components u, v translate with the expected speed without changing their shape, and neither dissipation nor dispersion was observed during the time evolution. In second place, we obtained numerically new periodic travelling wave solutions of the SBO system in a parameter's regime not covered by the theoretical results in previous works, suggesting that the regime of existence of such type of solutions of the SBO system can be extended to the case $w - c^2/4 < 0$.

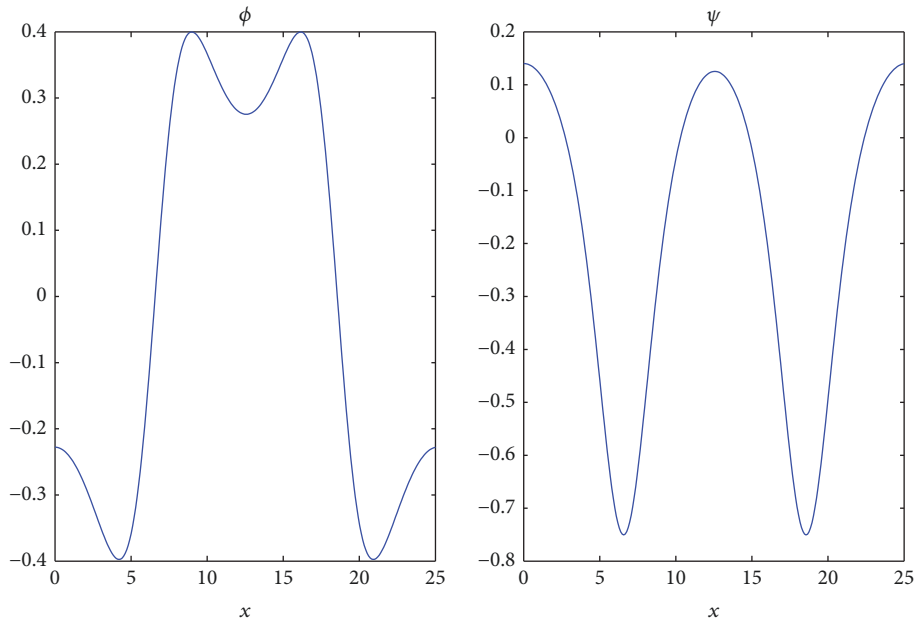

Figure 5: Approximations of the functions ϕ, ψ in the travelling wave solution (39) with 23 Newton's iterations. The model's parameters are $\alpha = \beta = \gamma = 1$, $\omega = 0.06$, and wave speed $c = 0.5$ and the fundamental period is $L \approx 25.13$.

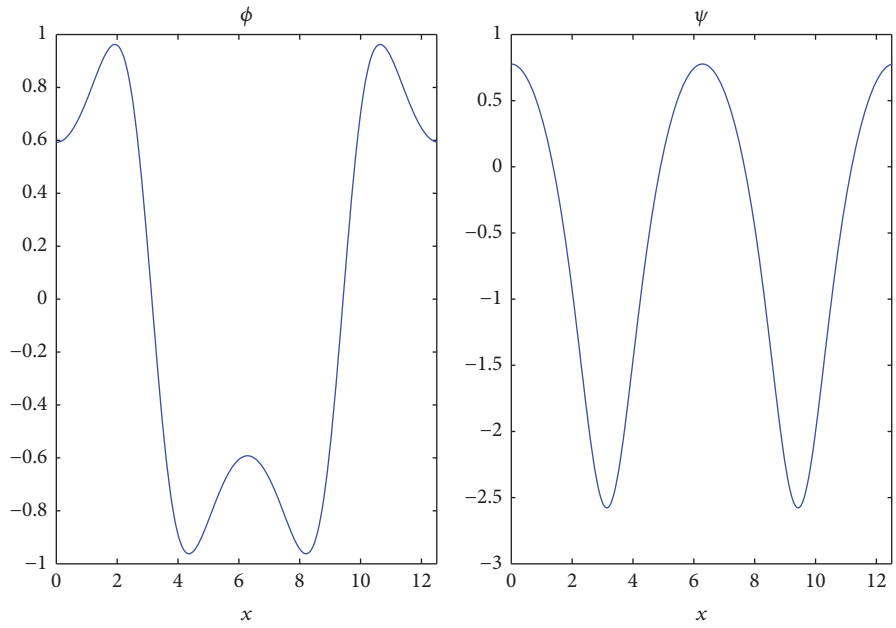

Figure 6: Approximations of the functions ϕ, ψ in the travelling wave solution (39) with 18 Newton's iterations. The model's parameters are $\alpha = \beta = \gamma = 1$, $\omega = 0.06$, and wave speed $c = 1$ and the fundamental period is $L \approx 12.57$.

Experiment Set 2 (Solitary Waves). In second place, we wish to compute approximations of solitary wave solutions of the SBO system. The following numerical simulations have the goal of showing that the proposed numerical solver is not restricted to the periodic case, and it can also be further employed to obtain approximations to solitary wave solutions of the SBO system on the real line, provided that the spatial computational domain is chosen large enough so that the solution does not reach the computational boundaries.

In this case, the functions ϕ and ψ and their derivatives must decay to zero at infinity. Thus, we run Newton's iteration to approximate the cero of the vector field given in (46) by using as initial step the solitary wave (19) corresponding to $\gamma = 0$. Here we set $\alpha = \beta = 0.4$, $\gamma = -1$, $c = 0.5$, $\omega = 1.5$, and $N = 2^8$ FFT points. We point out that Newton's scheme explained in the previous section is designed for searching spatial periodic solutions of the SBO system. However, due to the decay properties at infinity of a solitary

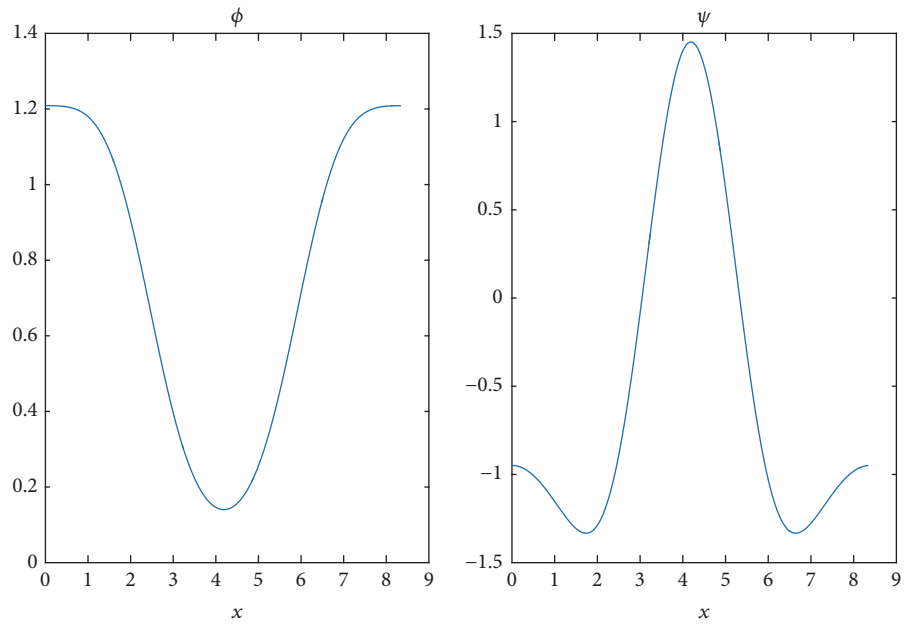

Figure 7: Approximations of the functions ϕ, ψ in the travelling wave solution (39) with 8 Newton's iterations. The model's parameters are $\alpha = \beta = \gamma = 1$, $w = 1.5$, and wave speed $c = 1.5$ and the fundamental period is $L \approx 8.38$.

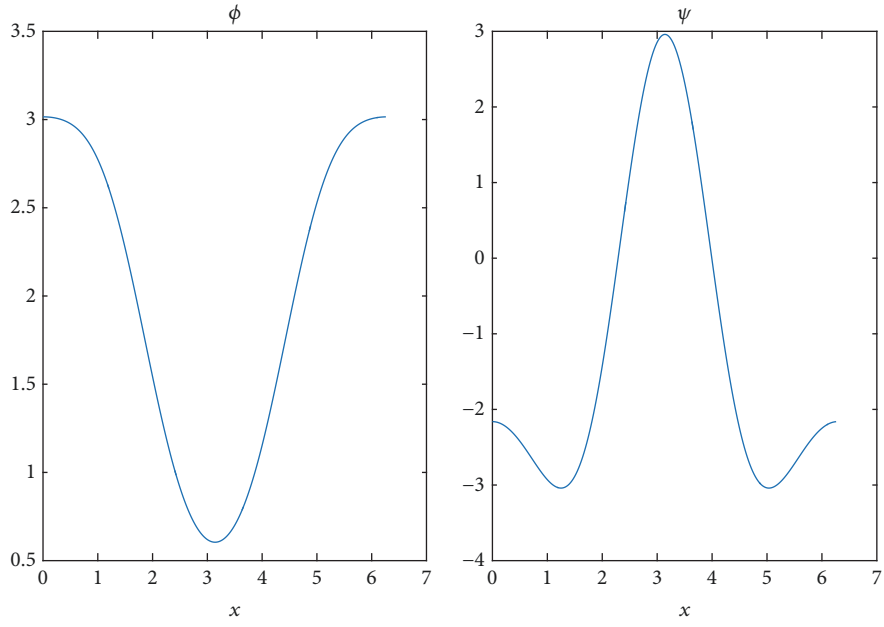

Figure 8: Approximations of the functions ϕ, ψ in the travelling wave solution (39) with 6 Newton's iterations. The model's parameters are $\alpha = \beta = \gamma = 1$, $w = 2$, and wave speed $c = 2$ and the fundamental period is $L \approx 6.28$.

wave solution, we can also use Newton's procedure adopting a spatial computational domain as the interval $[0, L]$ with L large enough. In this case we set $L = 120$. The result of this computer simulation is presented in Figure 9 and the corresponding verification that it corresponds really to a solitary wave solution of the SBO system is presented in Figure 10. In this validation we use the numerical parameters $\Delta t = 10^{-3}$ and $N = 2^{10}$ FFT points for the spatial discretization in the spectral numerical scheme introduced in [14]. The maximum error observed at $t = 40$ between the two wave profiles is roughly 10^{-4}. Other solitary wave solutions of the SBO system were computed for different values of the parameter w and the results are displayed in Figures 11, 12, and 13, for $w = 0.5$, $w = 0.1$, and $w = 0.07$, respectively. The parameters α, β, c, γ are the same as before. In the experiments in Figure 11, we use $L = 120$, $N = 2^8$, and for the experiments in Figures 12 and 13, we set $L = 400$, $N = 2^8$, and $L = 800$, $N = 2^{10}$, respectively. We recall that the wave component $v(x, t)$ of

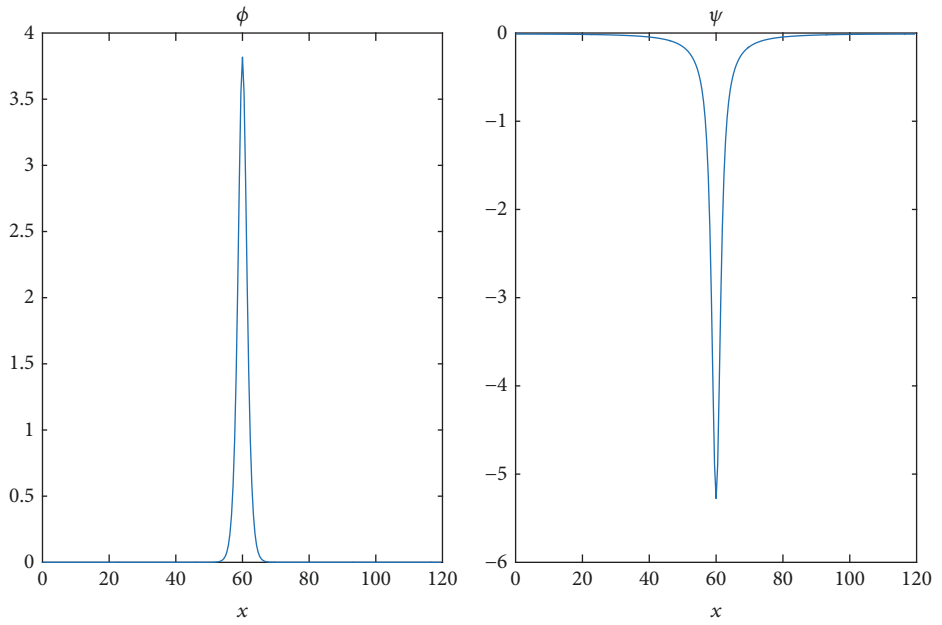

Figure 9: Approximations of the functions ϕ, ψ in the solitary wave solution (39) with 6 Newton's iterations. The model's parameters are $\alpha = \beta = 0.4$, $\gamma = -1$, $w = 1.5$, and wave speed $c = 0.5$.

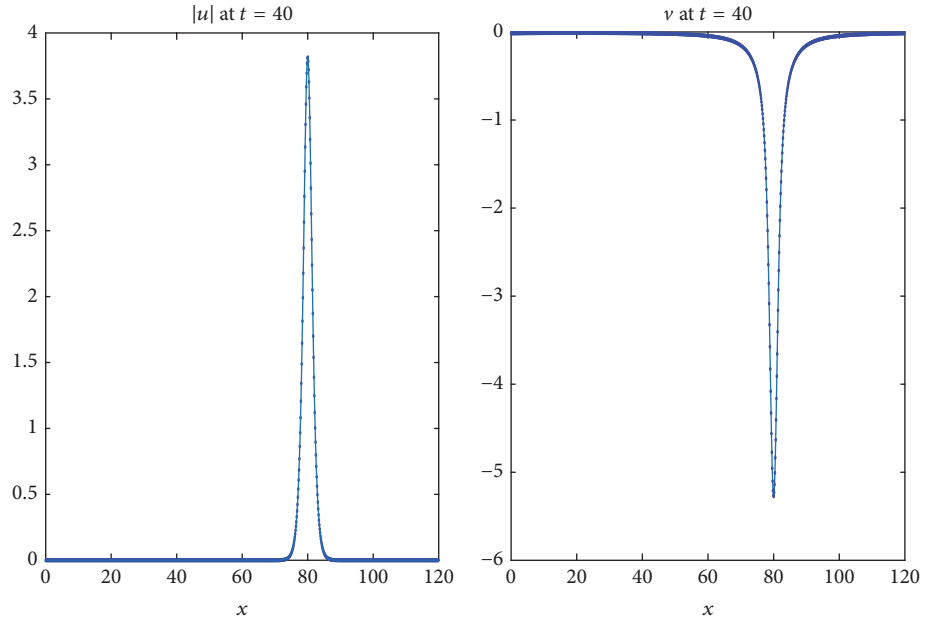

Figure 10: Evolution of a solitary wave solution (39) (with ϕ, ψ as in Figure 9) of the SBO system at $t = 40$. In solid line, $|u|, v$ computed with the numerical solver introduced in [14]. In pointed line, $|u|, v$ for the approximate solitary wave solution (39).

a travelling solution of the SBO system is given here by $v(x,t) = \psi(x - ct)$. Thus, observe that, in all solitary waves computed in this paper, the component $v(x,t)$ is negative. This is because solution (19) (corresponding to $\gamma = 0$) was adopted as the starting point for Newton's iteration in the case of solitary waves.

Experiment Set 3 (Influence of Model's Parameters). The previous numerical experiments illustrated the shape of some travelling wave solutions of the SBO system, not computed in previous works, to the knowledge of the author. In the next set of experiments, we wish to initiate the analysis of the dependence of the these travelling wave solutions (periodic and non periodic case) on the parameters appearing in the SBO system.

In Figure 14, we compare the computed periodic travelling waves for the SBO system for $\gamma = 0.6, 0.8, 1.0$. The rest of model's parameters are fixed at $\alpha = \beta = 1$, $c = 0.5$,

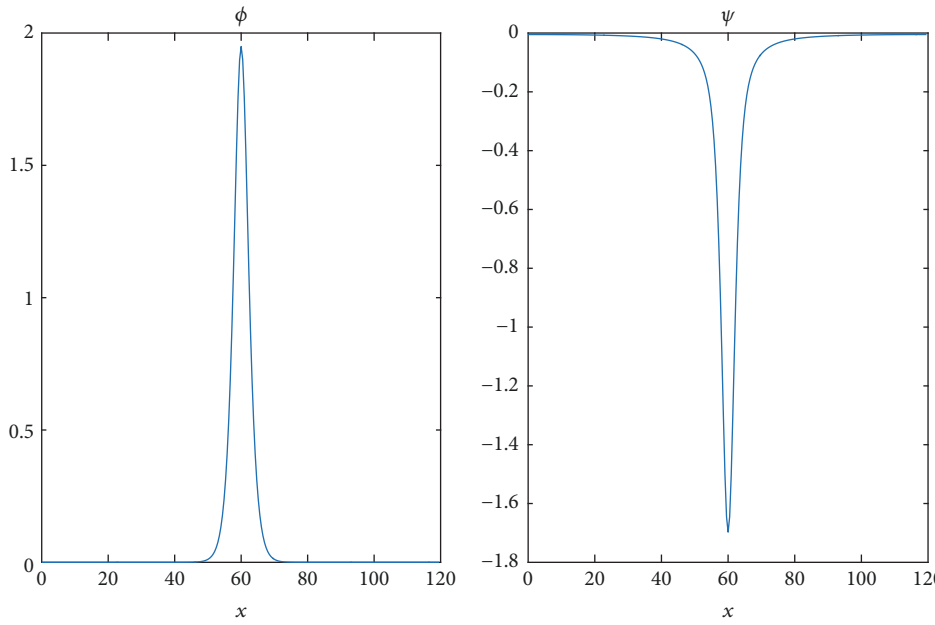

FIGURE 11: Approximations of ϕ, ψ in the solitary wave solution (39) with 6 Newton's iterations. The model's parameters are $\alpha = \beta = 0.4$, $\gamma = -1$, $w = 0.5$, and wave speed $c = 0.5$.

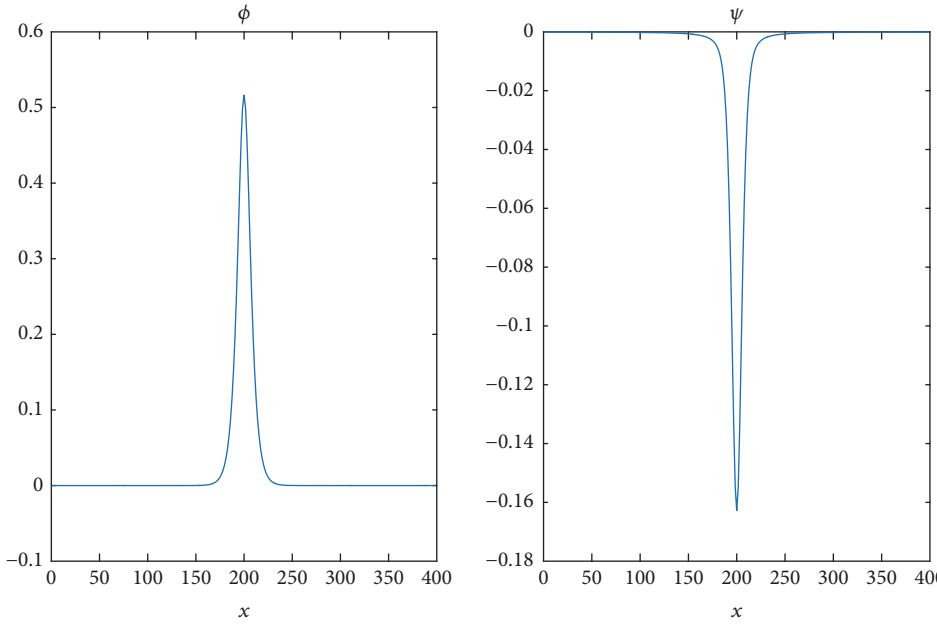

FIGURE 12: Approximations of the functions ϕ, ψ in the solitary wave solution (39) with 5 Newton's iterations. The model's parameters are $\alpha = \beta = 0.4$, $\gamma = -1$, $w = 0.1$, and wave speed $c = 0.5$.

and $w = 0.5$. From these computer simulations, we can see that the amplitudes of both components ϕ, ψ of the computed travelling wave increase when the parameter γ decreases. In contrast, in Figure 15, we explore the effect of the frequency w on the shape of the computed travelling wave. The parameters $\alpha = \beta = 1$, $c = 0.5$, and $\gamma = 0.5$ are left fixed. Notice that, in this case, the amplitude of the wave components ϕ, ψ results in being proportional to the value of the frequency w. In the case of solitary waves of the SBO system, we conducted similar numerical experiments to analyze the effect of the model's parameters γ, w on the amplitude of the computed profiles. The results are shown in Figure 16 (with $\alpha = \beta = 1$, $c = 0.5$, $w = 0.5$, and $\gamma = -0.1, -0.7, -1.0$) and Figure 17 (with $\alpha = \beta = 1$, $c = 0.5$, $\gamma = -1$, and $w = 0.4, 0.6, 1.0$). In contrast to the case of periodic waves, in this case the behavior of the solitary wave components ϕ, ψ differs from each other. For instance, notice that the amplitude of the component ϕ decreases when γ increases. Meanwhile, the component ψ

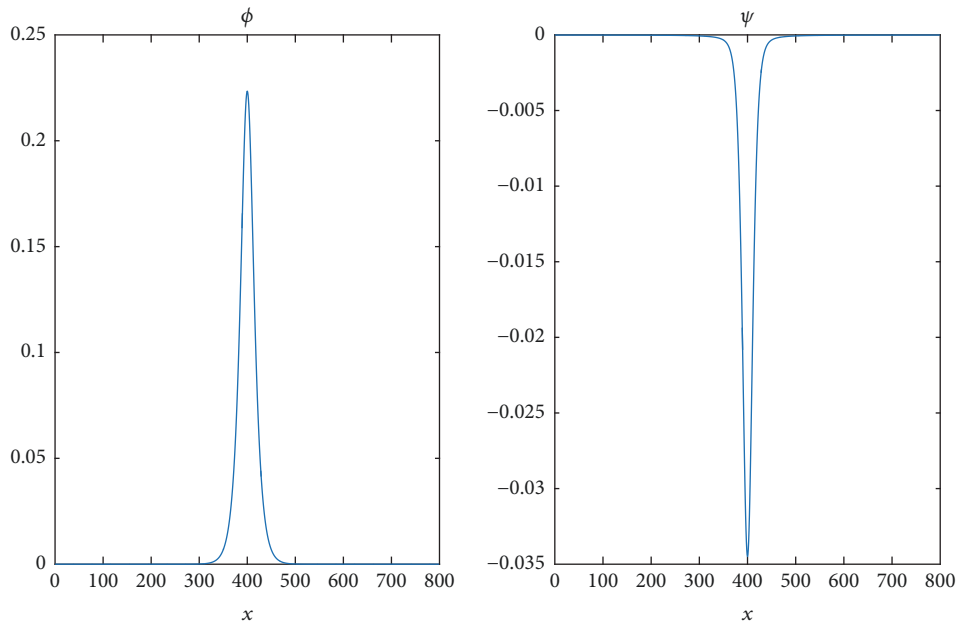

FIGURE 13: Approximations of the functions ϕ, ψ in the solitary wave solution (39) with 5 Newton's iterations. The model's parameters are $\alpha = \beta = 0.4$, $\gamma = -1$, $w = 0.07$, and wave speed $c = 0.5$.

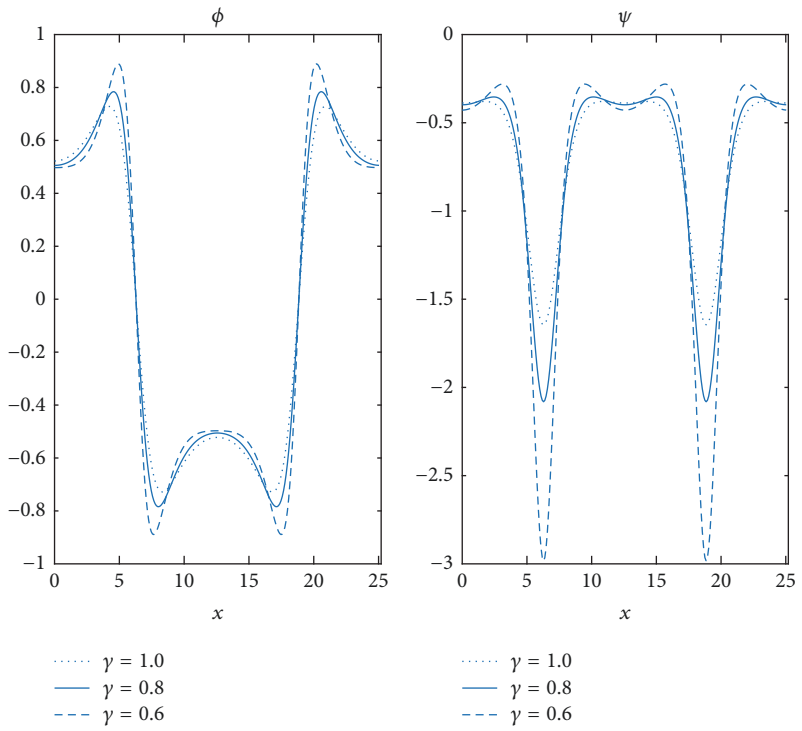

FIGURE 14: Comparison of periodic travelling wave solutions of the SBO system for different values of the parameter γ.

decreases its amplitude when γ decreases. Furthermore, the amplitude of both components ϕ, ψ is directly proportional to the frequency w.

To analyze the effect of the parameter α on the shape of travelling waves of system SBO, we conduct additional numerical experiments setting $\beta = 1$, $\gamma = 0.6$, $c = w = 0.5$, and $\alpha = 0.3, 0.4, 0.6, 1.0$. The resulting profiles computed with the Newton procedure are displayed in Figure 18. Observe that the amplitude of the computed travelling waves is inversely proportional to the parameter α. On the other

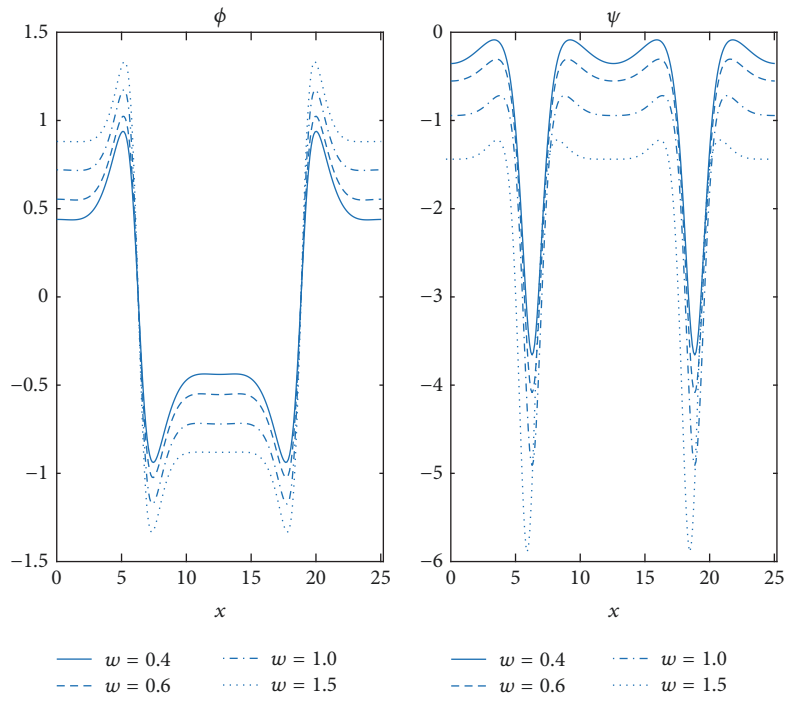

Figure 15: Comparison of periodic travelling wave solutions of the SBO system for different values of the frequency w.

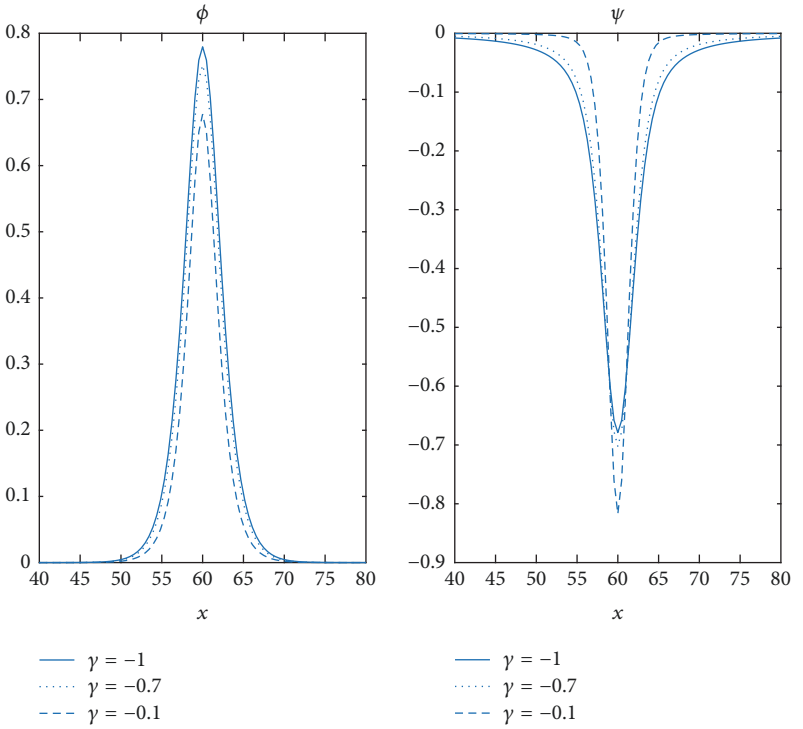

Figure 16: Comparison of solitary wave solutions of the SBO system for different values of the parameter γ.

hand, fixing $\alpha = 1$, $\gamma = 0.6$, and $c = w = 0.5$, we study in Figure 19 the influence of the parameter β. In these numerical experiments, we take $\beta = 2.8, 2.9, 3.0, 3.1$ and see that the corresponding travelling wave solution is more sensitive to changes of the parameter β (which alters the first derivative term $(|u|^2)_x$), in contrast to previous simulations varying the other parameters in the SBO system.

Experiment Set 4 (Solitary Wave Collisions). In this set of experiments we wish to explore the interaction between two

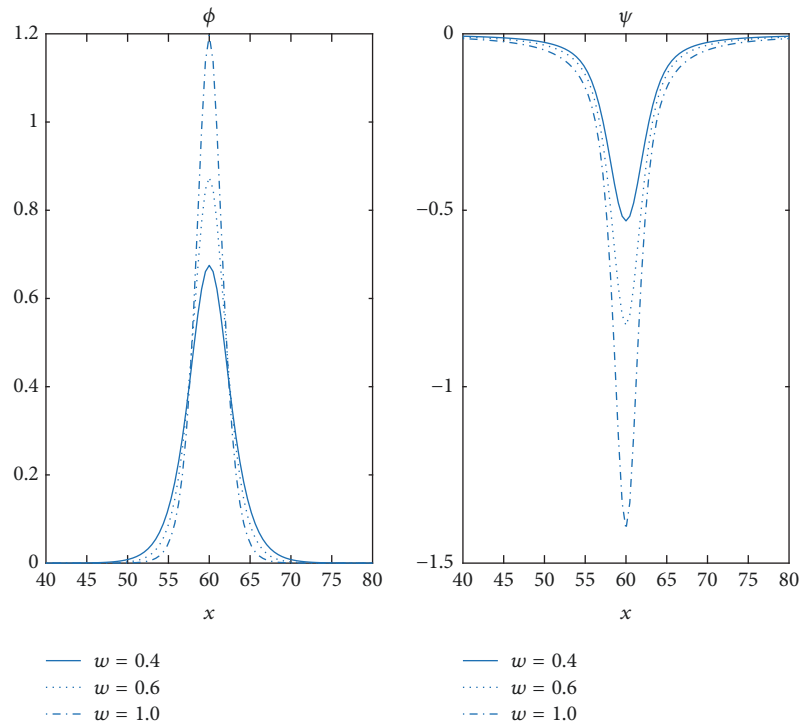

Figure 17: Comparison of solitary wave solutions of the SBO system for different values of the frequency w.

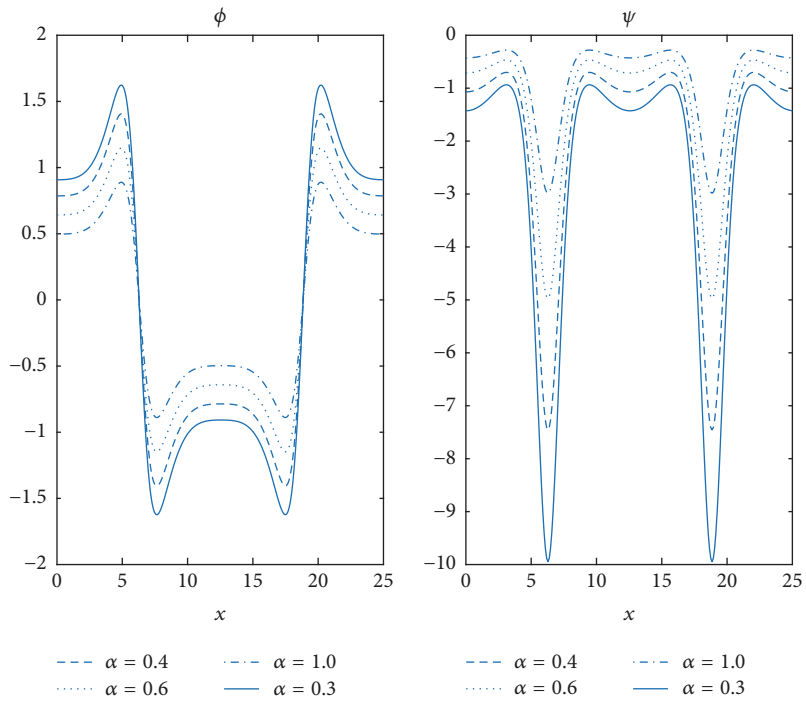

Figure 18: Comparison of periodic travelling wave solutions of the SBO system for different values of the parameter α.

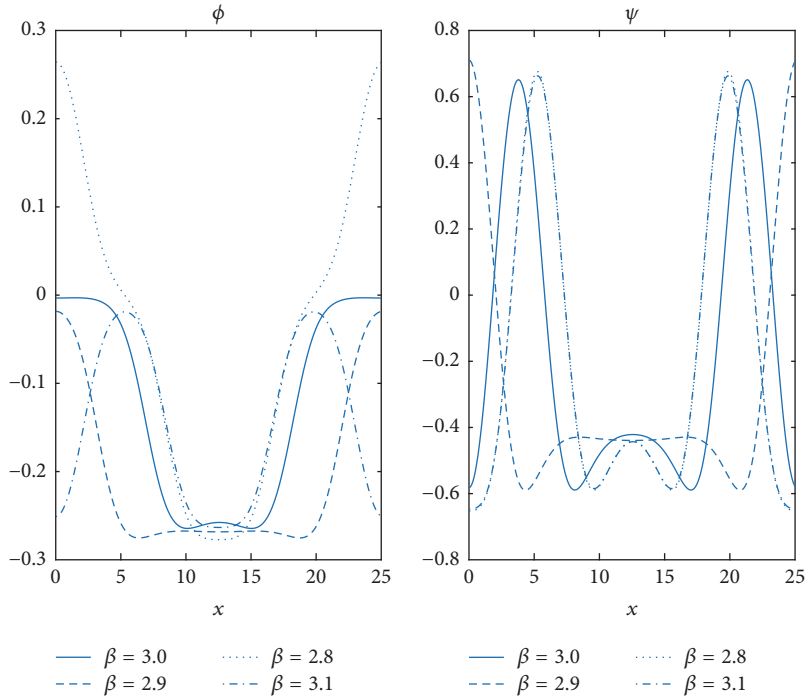

FIGURE 19: Comparison of periodic travelling wave solutions of the SBO system for different values of the parameter β.

solitary waves of system (1) with different speeds of propagation and amplitudes. As mentioned above, this phenomenon has not been considered in previous works on the SBO system, to the best of the author's knowledge. To do this, we compute the evolution of the initial profile

$$u(x,0) = e^{ic_1 x/2}\phi_1(x) + e^{ic_2(x-20)/2}\phi_2(x-20),$$
$$v(x,0) = \psi_1(x) + \psi_2(x-20), \tag{52}$$

where ϕ_1, ψ_1 are the solutions of (40) with wave speed $c = c_1 = 0.5$ and ϕ_2, ψ_2 are the solutions corresponding to wave speed $c = c_2 = 2$. The model's parameters for computing the profiles ϕ_i, ψ_i, $i = 1, 2$ are taken as $\alpha = \beta = 0.4$, $\gamma = -1$, and $w = 1.5$, and the spatial domain is the interval $[0, L]$ with $L = 120$. We point out that the profiles ϕ_2, ψ_2 have been moved to the right a distance of 20 units, so that the initial separation between the solitary waves is 20 units. Furthermore, the profile with a higher velocity $c_2 = 2$ is located behind the one with the lower velocity $c_1 = 0.5$. The numerical parameters are $\Delta t = 10^{-3}$ and $N = 2^8$ FFT points in this computer simulation. The results of the interaction of the two solitary waves are displayed in Figures 20 and 21, and in the contour plots shown in Figures 22 and 23, we can see the trajectory of each solitary wave in the $x - t$ plane before and after the collision. When $t \approx 10$ the larger solitary wave begins to shrink and the smaller solitary wave begins to grow. This process continues until the wave profiles have swapped identities, after which they separate. We always observe two local maxima in both components $|u(x,t)|$ and $|v(x,t)|$ during the entire interaction. When $t \approx 13$, the two solitary waves start to separate from each other. From these numerical experiments, we see that, before collision, the solitary wave with higher velocity $c_2 = 2$ moves towards the one with slower velocity $c_1 = 0.5$, with the expected speeds, and then one passes through another. We point out that, after collision, some small dispersive trailing waves are generated around the pulses. Then these tails separate from the solitary waves, lengthen, and become weaker progressively as time evolves. Further observe that the tails are the strongest for the wave component v, which is affected by the Hilbert operator in the second equation in the SBO system. We obtained similar results in other numerical simulations performed with different pairs of solitary wave solutions of the SBO system. This behavior is very different from that observed in other well-known integrable dispersive models, such as the Korteweg-de Vries equation [17], the Benjamin-Bona-Mahony equation [18], and the Benjamin-Ono equation [19], where the collision of two superimposed solitary-waves is elastic (i.e., clean, without forming dispersive tails). For the Benjamin-Ono equation, see also the numerical study of solitary wave collisions in the work by Thomeé and Vasudeva Murthy [20] and Pelloni and Dougalis [21]. We remark that this phenomenon has already been observed by Kalisch and Bona [22], who studied the interaction of solitary-wave solutions of the Benjamin-Ono equation, the regularized Benjamin-Ono equation, and the Benjamin equation, which are dispersive models where the Hilbert transform is also present. In accordance with that work, this behavior suggests that the SBO system is not integrable; that is, it does not have exact solitary-wave solutions, similar to the case of the Benjamin equation and the regularized Benjamin-Ono equation.

We point out that the parameter space for system (1) is large and thus, in this paper, we have presented only a limited

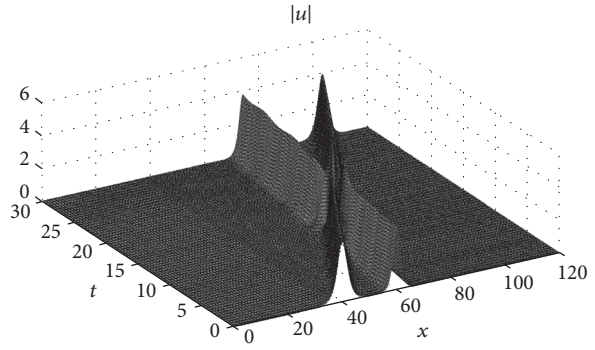

FIGURE 20: View in the x-t plane of the collision of two solitary waves of the SBO system with velocities $c = 0.5$ and $c = 2$. Observe that the colliding waves have different initial amplitude.

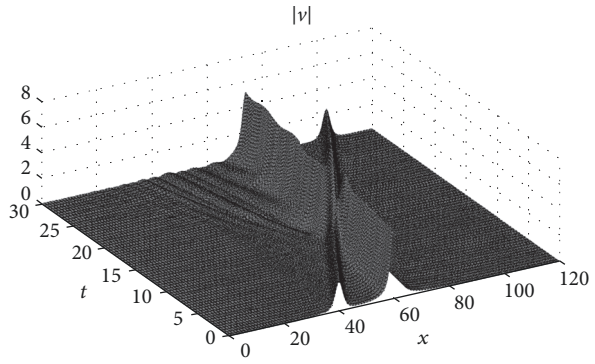

FIGURE 21: View in the plane x-t of the collision of two solitary waves of the SBO system with velocities $c = 0.5$ and $c = 2$. Observe that the colliding waves have different initial amplitude.

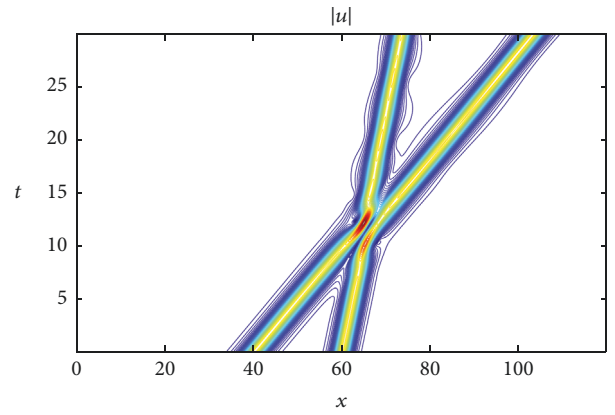

FIGURE 22: Wave-crest trajectory of collision of the two solitary waves of different speed and amplitude shown in Figure 20.

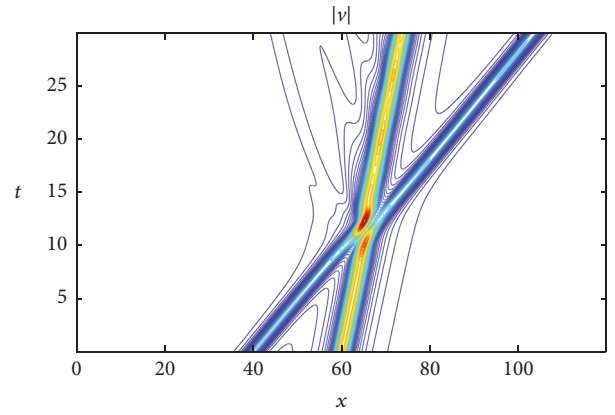

FIGURE 23: Wave-crest trajectory of collision of the two solitary waves of different speed and amplitude shown in Figure 21.

number of numerical experiments to illustrate the geometry of travelling wave solutions of the SBO system, in a parameter regime where no exact solution is known, and to initiate the study of interactions between these permanent wave states. Further numerical and analytical studies are necessary to determine the complete parameter space for existence of travelling waves to study important analytical properties, such as orbital stability, and to develop an exhaustive discussion of solitary wave interactions for the SBO system.

5. Conclusions

In this paper, we introduced a numerical scheme for approximating the travelling wave solutions (periodic and nonperiodic) of system (1), whose existence was established in previous works [7, 10, 13]. This scheme combines a Fourier spectral discretization together with a Newton-type iteration, using as initial step well-known exact solutions when $\gamma = 0$. Using the spectral Crank-Nicholson numerical scheme introduced by the author in [14] for approximating time evolution of solutions of the SBO system, we also illustrated the collision of two right-running unequal-amplitude solitary waves propagating with different speeds. The behavior of the colliding solitary waves was found to be similar to solitary waves of other well-known nonintegrable dispersive-type equations, such as the scalar regularized Benjamin-Ono equation and the Benjamin equation, for instance. As mentioned in the work by Kalisch and Bona [22], this phenomenon suggests that the SBO system is not integrable. Furthermore, we obtained numerically new periodic travelling wave solutions which are not included in the analytical theory presented in the work by Angulo et al. [13].

Conflicts of Interest

The author declares that there are no conflicts of interest regarding the publication of this paper.

Acknowledgments

This research was supported by Universidad del Valle, Calle 13, Nro. 100-00, Cali, Colombia, under Research Project C.I. 71020.

References

[1] M. Funakoshi and M. Oikawa, "The resonant interaction between a long internal gravity wave and a surface gravity wave packet," *Journal of the Physical Society of Japan*, vol. 52, no. 6, pp. 1982–1995, 1983.

[2] V. I. Karpman, "On the dynamics of sonic-langmuir solitons," *Physica Scripta*, vol. 11, no. 5, pp. 263–265, 1975.

[3] V. D. Djordjevic and L. G. Redekopp, "On two-dimensional packets of capillary-gravity waves," *Journal of Fluid Mechanics*, vol. 79, no. 4, pp. 703–714, 1977.

[4] R. H. J. Grimshaw, "The Modulation of an Internal Gravity-Wave Packet, and the Resonance with the Mean Motion," *Studies in Applied Mathematics*, vol. 56, no. 3, pp. 241–266, 1977.

[5] D. J. Benney, "Significant interactions between small and large scale surface waves," *Studies in Applied Mathematics*, vol. 55, no. 2, pp. 93–106, 1976.

[6] D. J. Benney, "General theory for interactions between short and long waves," *Studies in Applied Mathematics*, vol. 56, no. 1, pp. 81–94, 1977.

[7] J. Angulo and J. F. Montenegro, "Existence and evenness of solitary-wave solutions for an equation of short and long dispersive waves," *Nonlinearity*, vol. 13, no. 5, pp. 1595–1611, 2000.

[8] P.-L. Lions, "The concentration-compactness principle in the calculus of variations. The locally compact case. Part 1," *Annales De L Institut Henri Poincaré-Analyse Non Linéare*, vol. 1, no. 2, pp. 109–145, 1984.

[9] P.-L. Lions, "The concentration-compactness principle in the calculus of variations. The locally compact case. II," *Annales de l'Institut Henri Poincaré (C) Analyse Non Linéaire*, vol. 1, no. 4, pp. 223–283, 1984.

[10] J. Angulo Pava, "Stability of solitary wave solutions for equations of short and long dispersive waves," *Electronic Journal of Differential Equations*, No. 72, 18 pages, 2006.

[11] D. Bekiranov, T. Ogawa, and G. Ponce, "Interaction equations for short and long dispersive waves," *Journal of Functional Analysis*, vol. 158, no. 2, pp. 357–388, 1998.

[12] H. Pecher, "Rough solutions of a Schrödinger-Benjamin-Ono system," *Differential and Integral Equations. An International Journal for Theory & Applications*, vol. 19, no. 5, pp. 517–535, 2006.

[13] J. Angulo, C. Matheus, and D. Pilod, "Global well-posedness and non-linear stability of periodic traveling waves for a Schrödinger-Benjamin-Ono system," *Communications on Pure and Applied Analysis*, vol. 8, no. 3, pp. 815–844, 2009.

[14] J. C. Muñoz Grajales, "Error analysis of an implicit spectral scheme applied to the Schrödinger-Benjamin-Ono system," *International Journal of Differential Equations*, Article ID 6930758, Art. ID 6930758, 12 pages, 2016.

[15] T. B. Benjamin, "Solitary and periodic waves of a new kind," *Philosophical Transactions of the Royal Society of London. Series A. Mathematical, Physical Sciences and Engineering*, vol. 354, no. 1713, pp. 1775–1806, 1996.

[16] J. Angulo, M. Scialom, and C. Banquet, "The regularized Benjamin-Ono and BBM equations: well-posedness and nonlinear stability," *Journal of Differential Equations*, vol. 250, no. 11, pp. 4011–4036, 2011.

[17] T. R. Marchant and N. F. Smyth, "Soliton interaction for the extended Korteweg-de Vries equation," *IMA Journal of Applied Mathematics*, vol. 56, no. 2, pp. 157–176, 1996.

[18] T. B. Benjamin, J. L. Bona, and J. J. Mahony, "Model equations for long waves in nonlinear dispersive systems," *Philosophical Transactions of the Royal Society A: Mathematical, Physical & Engineering Sciences*, vol. 272, no. 1220, pp. 47–78, 1972.

[19] W.-R. Sun, B. Tian, H. Zhong, and R.-X. Liu, "Breather and double-pole solutions for the Benjamin-Ono equation in a stratified fluid," *Waves in random and complex media : propagation, scattering and imaging.*, vol. 26, no. 2, pp. 168–175, 2016.

[20] V. Thomeé and A. S. Vasudeva Murthy, "A numerical method for the Benjamin-Ono equation," *BIT Numerical Mathematics*, vol. 38, no. 3, pp. 597–611, 1998.

[21] B. Pelloni and V. A. Dougalis, "Numerical solution of some nonlocal, nonlinear dispersive wave equations," *Journal of Nonlinear Science*, vol. 10, no. 1, pp. 1–22, 2000.

[22] H. Kalisch and J. L. Bona, "Models for internal waves in deep water," *Discrete and Continuous Dynamical Systems - Series A*, vol. 6, no. 1, pp. 1–20, 2000.